

External anode mortar with superior performance based on lightweight functional aggregates for Impressed Current Cathodic Protection of reinforced concrete

Wenhao Guo ¹, Jie Hu ^{1,2}, Suhong Yin ^{1,2}, Jiangxiong Wei ^{1,2}, Qijun Yu ^{1,2}

¹ School of Materials Science and Engineering, South China University of Technology, Guangzhou, Guangdong, China

² Guangdong Low Carbon Technologies Engineering Center for Building Materials, Guangzhou, Guangdong, China

Cathodic protection has proved to be an effective and reliable technique for the corrosion protection of reinforced concrete structures, especially in chloride-contaminated environment. However, its application can be constrained by unsatisfactory anode service life [Weale, 1992]. Many shortcomings reported in the literatures were related to low and non-uniform distributed conductivity and degradation of anode systems, mainly their cementitious overlay, due to the acidification in the vicinity of the anode metal during the treatment [Page, 2000]. Based on this electrochemical characteristic issue, the ideal anode overlay was suggested to be equipped with good ionic conductivity and possibly moderately influenced by the environmental humidity variations [Pedferri, 1996]. In this paper, a novel type of lightweight functional aggregate (CA) was prepared by impregnating an alkaline modified agar solution (changed into a solid gel after cooling) into the porous structures of ceramsites. An external anode mortar with superior performance was then prepared based on these functional aggregates, aiming at improving the conductivity of the mortar embedding the anode and halting the negative effects induced by anodic reactions. On one hand, the resistivity of the prepared conductive mortar in the presence of CA was in the range from 15.3 to 14.2 Ωm at the curing age of 28 days, basically 70% lower than plain mortar prepared with 45 vol.% of river sand. The high conductivity was related to the establishment of an effective conductive network formed by CA. On the other hand, the capacity for maintaining an alkaline environment was improved by 53% - 132% in presence of 15 ~ 40 vol.% of CA compared to that of the reference specimen. Meanwhile, the presence of CA in anode cell also

contribute to the maintenance of catalytic activity in low polarizing state (0.6–0.8 V vs. SCE), which was beneficial for the long term performance of anode system.

Keywords: External anode mortar, lightweight functional aggregates, conductivity, acidification erosion, cathodic protection

1 Introduction

The degradation of reinforced concrete (RC) structures induced by steel corrosion, especially for those operating in chloride-containing environment, has now been found to be one of the most serious durability problem constraining the expected service life of infrastructures [Bertolini, 2013]. Among all the available corrosion protection techniques, impressed current cathodic protection (ICCP) has been proved to be an effective technique for the corrosion protection of reinforced concrete structures, especially in chloride-contaminated environment [Pedferri, 1996]. ICCP systems mainly consist of three parts: a direct current (DC) power supply, a cathode system (reinforcement), and an anode system [Koleva, 2007], among which the anode is a very important component. The applied anode system may vary based on the specific protection requirements of RC structures [Bennett, 1993], but most of them can be characterized as an anode metal embedded in a cementitious overlay [Pedferri, 1996]. During ICCP treatment, the following anodic reactions will happen at the anode/concrete interface [Bennett, 1993]:



The above reactions will consume OH^- in alkaline pore solution and further cause acid dissolution damage in the vicinity of primary anode [Pedferri, 1996] and reduced service life of anode system [Peelen, 2008].

Moreover, in order to guarantee a relatively uniform polarization state, normally a high conductivity for the secondary cementitious anode material is required. In this respect, various types of conductive enhancing components, e.g. carbon black [Monteiro, 2015], steel shavings [Yehia, 2000] or carbon fibers [Xu, 2011] were admixed to cement-based anode materials. Carbon fibers were the most effective materials; however, the difficult

dispersion [Garcés, 2012] may lead to compromised modification effects [Gao, 2012] or even non-uniform distribution of protection current and reduced protection efficiency. In this paper, a novel type of lightweight functional aggregates (CA) was designed and prepared by impregnating an alkaline modified agar solution into ceramsites, a kind of porous structure contained expanded particles that prepared with mainly sludge or clay by sintering. An anode embedding mortar with superior performance was then prepared based on the lightweight functional aggregates: on one hand, the pre-stored alkali ions will release from the modified agar gel in the aggregates to maintain the alkaline environment in the anode mortar, thus reduced the acidification erosion damage induced by the anodic reaction; on the other hand, the admixed conductive aggregates may increase the total volume fraction of the conductive phase and contribute to the formation of a conductive network compared to conventional siliceous aggregates, thus leading to a better polarization uniformity of the total anode system.

2 Experiments

2.1 Materials

In this study, ordinary Portland cement P II 42.5 (the chemical composition is shown in Table 1) and local tap water was used to prepare the mortar specimens. Two types of aggregate were applied in this study: the lightweight functional aggregates (CA) and conventional siliceous aggregates (NA).

Table 1: Chemical composition of P II 42.5 Portland cement (wt.%)

Composition	SiO ₂	Al ₂ O ₃	Fe ₂ O ₃	CaO	MgO	K ₂ O	Na ₂ O	SO ₃	TiO ₂	rest
Content	21.86	4.45	2.35	63.51	1.67	0.55	0.26	2.91	0.11	2.33

Agar powders (C₁₂H₁₈O₉)_n used in this study was plant tissue culture grade with a gel strength of 1300 g/cm² (code: H8145), porous ceramsites and analytical grade reagents e.g. NaOH, Ca(OH)₂ and KOH were applied in the preparation of CA. Chemical compositions and basic physical characteristics of porous ceramsites were given in Table 2.

For the resistivity measurements of mortar samples, titanium mesh electrodes were embedded in mortar bars as electrode in a 4-point direct current (DC) test.

Table 2: Chemical composition (wt.%) and physical characteristics of porous ceramsites

SiO ₂	Al ₂ O ₃	Fe ₂ O ₃	CaO	MgO	K ₂ O	Na ₂ O	MnO	P ₂ O ₅	TiO ₂	SO ₃
52.92	20.84	13.39	6.13	0.99	2.83	0.66	0.45	0.19	0.95	0.15
Physical characteristics of porous ceramsites										
Bulk density		1h water absorption		Cylinder compressive strength				Size range		
0.40 g/cm ³		11.00%		2.20 MPa				1.00~6.00 mm		

Table 3: Compositions of simulated concrete pore solution

Ca(OH) ₂	NaOH	KOH	NaCl	pH
0.002 mol/L	0.06 mol/L	0.18 mol/L	3.0 wt.%	13.29

In addition, concrete prisms were cut with dimensions of 40 mm × 30 mm × 20 mm from the formed surface of C30 strength grade concrete cubes, and the related mixture design and curing condition are listed in Table 4.

Table 4: Mixture proportions (kg/m³) and curing condition of the concrete sample

Water	Cement (P II 42.5)	Slag	Fly ash (secondary)	Fine aggregates (silica sand)	Coarse aggregates (crushed limestone)	Superplasticizer
173.8	246.0	70.0	35.0	741.0	1631.0	2.3

Note: the particle size range of coarse aggregate is 5-20 mm, the applied superplasticizer is polycarboxylate superplasticizer with a solid content of 30%

Curing condition: Moist-cured at ambient temperature for 6 month before cutting

2.2 Sample preparation

2.2.1 Preparation of CA

The CA was prepared by impregnating modified agar gel solution into dry and preheated porous ceramsites (100 °C). Specific parameters and proportion of all components for the preparation were as presented in Table 5. The uniform distribution of Ca(OH)₂ and graphite powder (further increase the conductivity of the gel) in the solution was achieved under the mixing condition. The ceramsites should be pre-heated to 90 ± 5 °C before this impregnation treatment, and the ceramsites should be completely submerged in the

modified agar solution and mixing for 2 minutes. After that, the mixture was stewed and cooled to room temperature to achieve the gelation. The load ratio, defined as the mass of modified agar gel that impregnated during this treatment and the mass of the raw ceramsites before treatment, was calculated with the following equation:

$$w = \frac{m_x - m_0}{m_0} \times 100\% \quad (4)$$

in which w is the load ratio (%); m_x is the mass of ceramsites after impregnating treatment (g); m_0 is the mass of raw ceramsites (g); the calculated load ratio of CA was within the range of 38%~49%.

Table 5: Mixture and preparation procedures of the modified agar gel solution

Procedure No.	Stirring speed (r/min)	Material added (g/100ml)	Time (min)/Temp (°C)
1	30	Water/100.0	--/100.0
2	30	Agar powder/6.00	10.0/100.0
3	30	NaOH/0.33	0.5/90.0
4	30	KOH/1.40	0.5/90.0
5	60	Ca(OH) ₂ /8.62	1.0/90.0
6	120	Graphite/5.00	1.0/95.0

2.2.2 Preparation of conductive mortar

To investigate and verify the effect of the prepared CA on the conductivity of cement-based materials, mortar samples were prepared with constant water to cement ratio ($w/c = 0.4$) and varied volume fraction of aggregate component ranging from 0.0 vol.% to 45 vol.% (relative to the overall volume of mortar samples). The applied aggregate size range is 3.5 mm to 4 mm.

The dimensions of mortar samples were 40 mm × 40 mm × 160 mm. There were three replicates for each specimen. 4 pieces of Ti mesh electrodes were inserted at the specific locations as presented in Figure 1 for the electrical resistivity measurement. All prepared cementitious specimens were cured at 20 ± 2 °C and relative humidity of 95% till certain curing ages (3/7/14/28/35 d respectively).

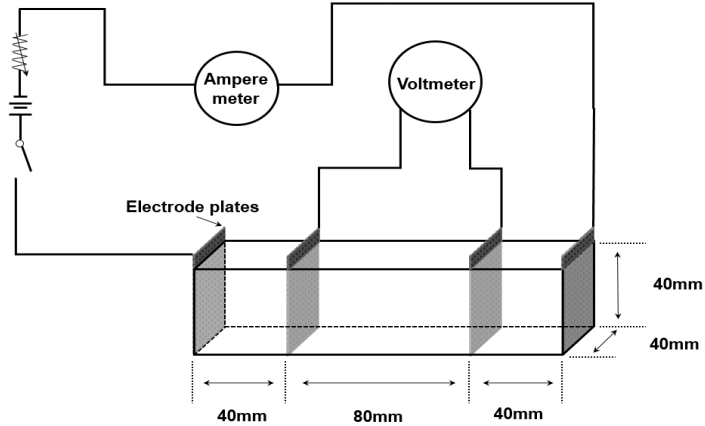


Figure 1: Schematic diagram of mortar samples and resistivity measuring operation

2.2.3 Preparation of simulated ICCP cells

The experimental setup for the quantitative characterization of the acidification process in the anode system is shown in Figure 2. The simulated concrete solution in both cathode and anode cells was prepared following the chemical compositions presented in Table 3. The designed exposed area of the titanium anode was 63 mm². The area ratio between the exposed concrete surface and primary anode surface was 19.0, which is similar to the

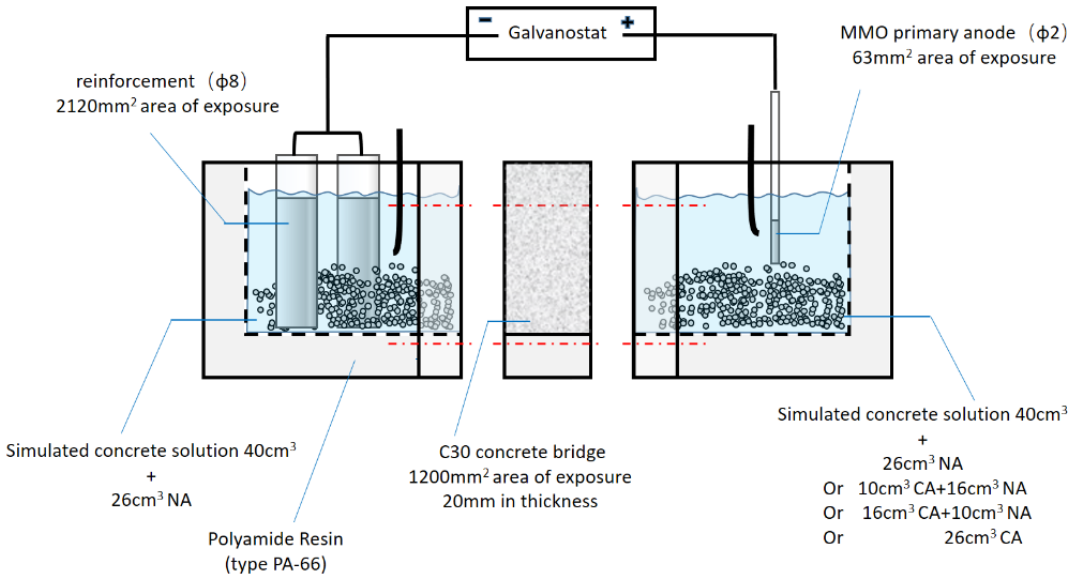


Figure 2: Schematic diagram of simulated ICCP experimental device

values reported in the literature (20.0) [Bertolini, 2004]. The exposed concrete surface was polished with no.60, no.220 and no.600 grinding papers on a lapping plate with a speed of 200 rad/min. Both cells were then assembled with the concrete bridge using epoxy resin. It should be noted that the formed face of the concrete bridge was facing the anode cell to present conditions as close as possible to an actual ICCP system. 3 replicates were prepared for each group of aggregate design.

2.3 *Methods*

2.3.1 *Electrical resistivity measurement*

The electrical resistivity of the conductive mortar was measured by 4-point DC method, and the detail information of the arrangement and setup can be referred to ASTM G57-06(2012).

The resistivity of concrete bridge in the simulated ICCP experimental device was calculated by the following equation:

$$\rho = \frac{US}{IL} \quad (5)$$

in which I is the applied current (A); U is the potential difference between the anode and cathode cells vs. SCE reference electrodes (V); S is the exposed surface area of the concrete bridge (m^2); L is the thickness of the concrete bridge (m).

2.3.2 *Galvanostatic tests for simulated ICCP cells*

The positive and negative terminals of the galvanostat (Corrtest CS1002) were connected to reinforcement and anode wire respectively. A constant current of 422 μA was then imposed for each simulated ICCP cell, which equates to 200 mA/m^2 of current density referred to the cathode, and 6700 mA/m^2 of current density referred to the MMO anode surface. The current density referred to the concrete surface area was 350 mA/m^2 . There were 3 replicates for each specimen.

2.3.3 *pH monitoring of anode cell*

To monitor the acidification process in anode system during the accelerated simulated test, 8-10 ml solution from anode cell was collected for the pH measurement by Mettler Toledo FE20K pH meter. The collected solution was then re-filled to the cell after the measurement.

2.3.4 Anode potential monitoring

The potential of the anode wire was measured periodically against a saturated calomel electrode (SCE), off-potential was not measured in this test.

2.3.5 Potentio-dynamic polarization (PDP) measurements

After the ICCP test was terminated and the anode potential was stable, a conventional three-electrode set-up was applied for the PDP measurement in the anode cell with the acidized pore solution; MMO anode wire as working electrode (WE), saturated calomel electrode as reference electrode (RE) and Ti mesh as counter electrode (CE). The scanning potential range for PDP was -0.2~1.0 V vs. OCP, with a scanning rate of 0.5 mV/s.

2.3.6 Light microscopy and image analysis

Image analysis was carried out with images obtained by light microscopy (Olympus SZX10) with a magnification of 3.15x to investigate the morphology of impregnated CA particles and the distance between CA in mortar specimens. For the observation of the internal pore structure of porous ceramsite particles, due to the impregnated agar gel was very easy to be destroyed during cutting, they were impregnated within epoxy resin with fluorescent dye (EpoFix pack, Struers Ltd), the dye contained epoxy resin was adjusted to the same viscosity compared with that of modified agar solution to simulated the impregnation treatment. The dye contained epoxy resin would then penetrate into the open pores of the ceramsites just like the way agar gel solution did during the impregnation treatment. After hardening for 48 h, the sample was then cut to present the cross sectional surface for a second impregnation with epoxy resin contained no fluorescent dye. The close pores would be opened during the cutting and the second epoxy resin impregnation was for the strengthen of porous structure additionally to ensure the porous structure did not break during the following polishing treatment. The hardened cutting surface of ceramsite particles was then polished with no. 320, no. 500, no. 800 grinding papers.

For the observation of aggregate spacing, the cross sections of mortar specimen were cut and polished with no. 320, no. 500, no. 800 grinding papers and then dried in oven at 90 °C until the weight of the samples maintained constant. For each specimen, 15 images were used for the image analysis, and at least 50 aggregates were selected to evaluate the distance between aggregate particles. GetData Graph Digitizer 2.22 was applied to measure and record the distance between aggregates.

3 Results and discussions

3.1 Morphology of the prepared CA

The internal structure of an impregnated CA particle is shown in Figure 3. Based on image analysis, the total porosity of ceramsites was up to 48%, providing sufficient space for the impregnation treatment. More importantly, agar gel can be successfully loaded into the porous air voids (evident by the fluorescence effect). The relatively large volume fraction of open pores indicated that modified agar gel component can be impregnated into the ceramsites and the composite is expected to have modified conductivity and provide supplementary ions for the maintenance of high alkaline environment in the anode cell solution. Related test and analysis were discussed in the following sections.

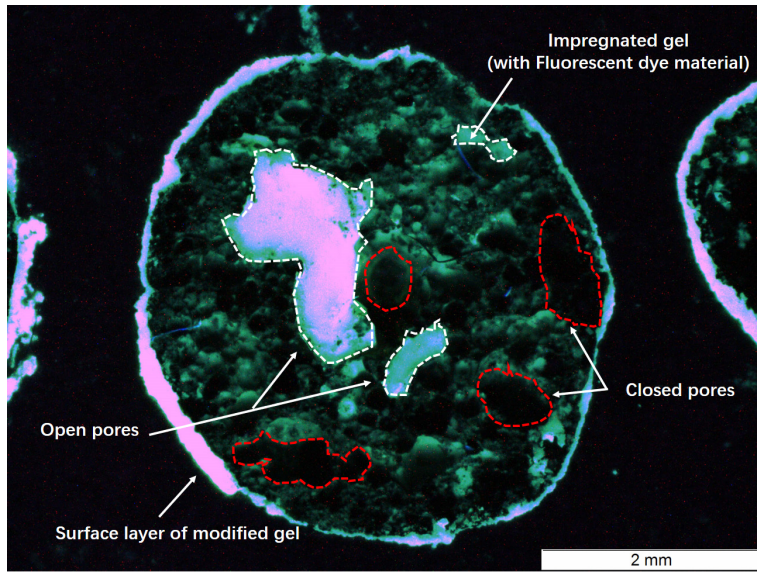


Figure 3: Internal structure of lightweight functional aggregate (CA)

3.2 The influence of functional aggregates on the electrical resistivity of mortar

The electrical resistivity of conductive mortar specimens with varied amount of CA is presented in Figure 4. It can be observed that the resistivity of the conductive mortar was significantly improved by the admixed CA, and a lower resistivity was related to a higher volume fraction of CA. For example, at a curing age of 28 d, the resistivity of mortar was around 25 Ωm for the specimens without CA, 21 Ωm for the specimens with 20 vol.% CA, 15 Ωm for the specimens with 40 vol.% CA and 10 Ωm for the specimens with 45 vol.% CA,

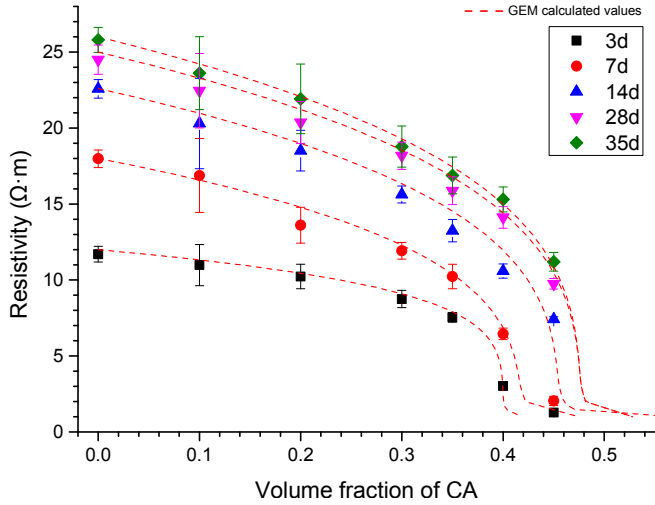


Figure 4: Resistivity of conductive mortar specimens with different amount of CA

respectively. The resistivity of all mortar specimens presented the smallest variation at a curing age of 28 d, indicating that the conductive structure was basically stable after 28 days curing.

For mortar specimens with 45 vol. % CA, the measured resistivity was $9.70 \Omega\text{m}$ at a curing age of 28 d, which was 60% lower, compared to cement paste without CA ($24.5 \Omega\text{m}$). Moreover, all measured values can be explained by the general effective media (GEM) model [McLachlan, 1990] and calculated by related equations.

3.3 Contribution of CA on the formation of conductive network in mortar

The modification effect of CA on the conductivity of mortar is different from carbon fibers. It was extensively reported that when carbon fibers were admixed in cement-based materials, a percolation threshold of carbon fibers was observed to achieve a low resistivity [Xu, 2011 & Wen, 2007]. However, when CA was used, the modification was a more gradual process as presented in Figure 4. This is considered to be related to the increased ionic conduction induced by CA, to be more specific, a higher volume fraction of conducting phase would result in a modified overall conductivity.

The distance (spacing) between conductive aggregates in mortar specimens obtained from image analysis is shown in Figure 5. The measured distance between CA particles gradually decreased: in conductive mortar with 10% CA, the distance between CA was in

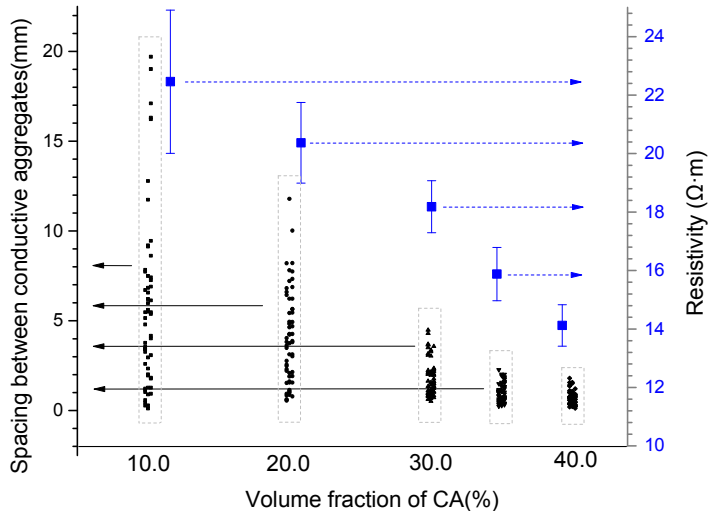


Figure 5: Distance among conductive aggregates in mortar specimens

the range from 0.1 mm to 20 mm; however, in conductive mortar with 40% CA, the distance between CA was in the range from 0.1 mm to 1.5 mm.

Generally, with a small distance, the conductive network in mortar can be more easily established by CA with a lower resistivity compared to cement particles and hydration products. Therefore, when the addition of CA was increased, the resistivity of mortar was gradually reduced.

3.4 The influence of functional aggregates on the acidification process in the anode system

As presented in Figure 6, the monitored voltage of all test ICCP cells varied with the treatment time. Relatively big differences in cell voltage can be observed between ICCP samples. A possible explanation to this phenomenon is the insufficient micro-scaled structural uniformity of the concrete bridge. However, the majority of test cell voltage increased with the extending of ICCP treatment time after operating for 15 days.

Considering the fact that the anode potentials were within the range of 1.2 to 0.6 V vs. SCE and those of cathode were within the range of -0.6 to -1.1 V vs. SCE, the majority of the cell voltage was distributed to the concrete bridge. Therefore, the variation in the total cell voltage can be attributed to the micro-scaled structural alteration of the concrete bridge (which will be discussed in the following section).

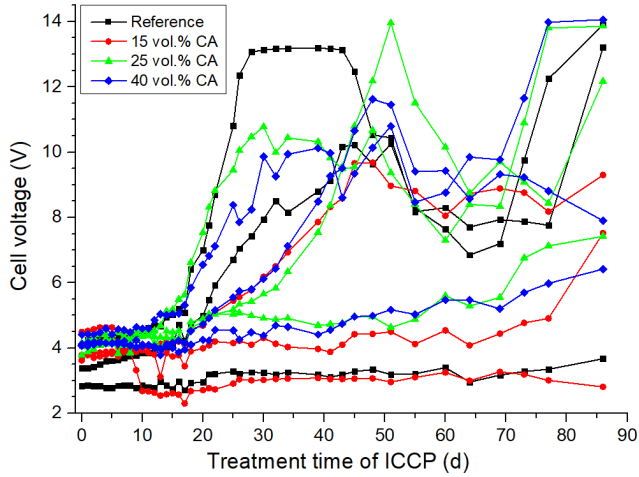


Figure 6: Monitored voltage of all test ICCP cells

The pH values of simulated concrete pore solution in the anode cell are presented in Figure 7. It can be observed that all anode cells suffered from acidification caused by the anodic reaction: a distinct drop of pH of the (simulated concrete pore) solution was observed in all test cells owing to the occurrence of Equations 1-3. However, with the increasing volume fraction of CA in the anode cell, the acidification process was slowed down. When the precipitation-solubility equilibrium between OH^- in concrete pore solution was broken by acid, hydration products would dissolve to replenish the consumed hydroxyl ions. Normally, the dissolution order of hydration products in cement-based materials would be expected to be: CH, AFm, Aft, C-S-H gels [Adenot, 1992]. Therefore, the equilibrium pH value of saturated calcium hydroxide (12.65), can be regarded as the critical point for the beginning of the dissolution of hydration products due to anodic reactions.

As presented in Figure 7, the beginning of CH dissolution happened after the electrode was energized for an accumulative electric charge quantity of about 620 C for the reference specimen (without CA); however, the accumulative electric charge was extended to about 950 C, 1170 C and 1420 C for the specimens with 15%, 25% and 40 vol.% CA, respectively. The above results indicate that the prepared CA in this study can efficiently increase the buffer capacity of high alkaline environment of simulated pore solution in the anode cell. Generally, the anodic reactions would consume the main reactive ion in the surrounding environment and thus compromised the catalytic efficiency. In this respect, a higher buffer capacity of high alkaline environment in the presence of CA provide the catalytic

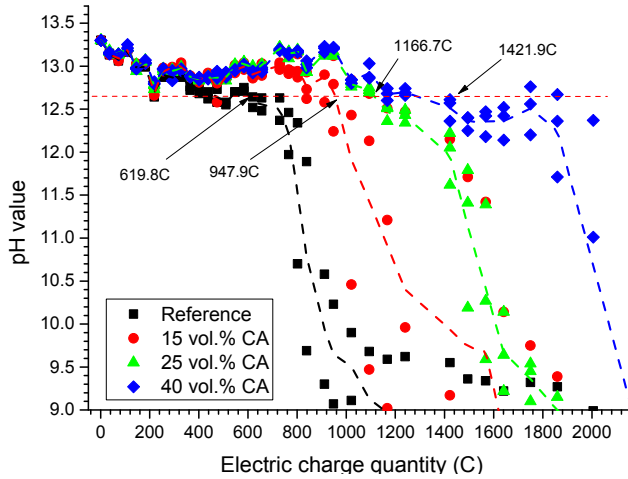


Figure 7: pH values of simulated concrete pore solution in anode cell in simulated ICCP experiments

environment with extra moles of OH⁻, which is beneficial for the catalytic efficiency of the primary anode, and thus result in lower anodic polarization potential in constant current operating state.

3.5 Effect of CA on polarisation of the anode XX

The potential of the MMO-coated titanium anode during the test is shown in Figure 8. The fluctuation in on-potential can be explained by the precipitation and elimination of generated oxygen bubbles, a gradual increasing trend in anode on-potential of all specimens can be observed in Figure 8. The relative large scaled increasing in anode potential was close to the time point of anode acidification in reference cells: the average anode potential increased from 822.0 mV vs. SCE (after energized for 546.9 C) to 1103.5 mV vs. SCE (after energized for 838.6 C). This variation is resulted by the consumption of the reactive ions in anode cell, mainly hydroxyl, thus constraining the acquisition of an appropriate reaction conditions with the preceding polarization level. To keep the constant current of the anode cell, a higher potential must be applied to the primary anode. The acidic erosion results that observed in Figure 8 also supports the above analysis: anode cell pH dropped sharply after energized for 619.8 C, approximately the same time with the increasing of anode potential. However, the increase of anode potential was less obvious for the specimens with CA, meaning that the prepared CA can guarantee the stable

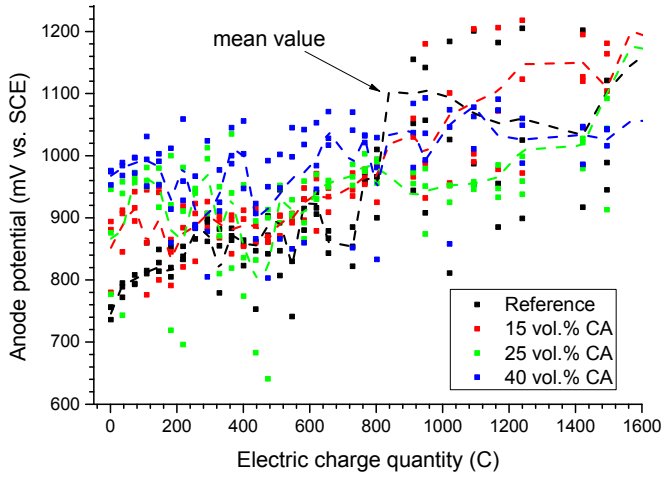


Figure 8: Potential of the primary anode in simulated ICCP experiments

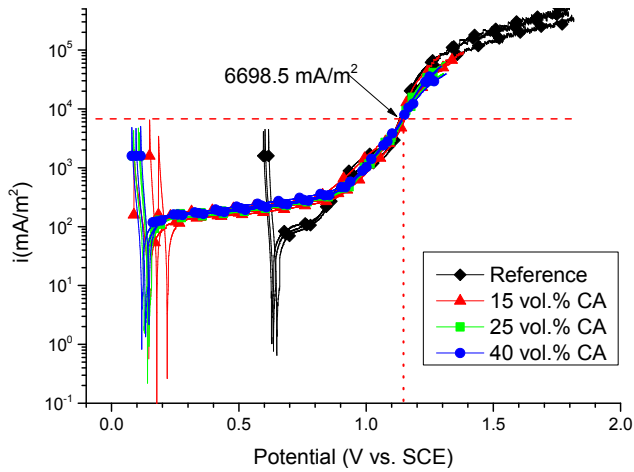


Figure 9: PDP curves of primary anode after energized for 3135.6 C

operation of ICCP treatment. The alkaline buffer capacity of CA in the anode cell was also beneficial for obtaining more stable operation conditions of the anode.

As a result, the difference in anode acidification process also led to the distinction in the performance of primary anode material. Figure 9 shows the PDP curves of primary anode for different specimens after ICCP treatment. The same polarizing effects of anode cell (above 0.8V vs. SCE) with or without CA would obtain the same level of anodic current

density (above 400 mA/m²). Even though the catalytic performance of all primary anode in high current density condition had almost no difference, the catalytic efficiency presented different features in low polarization interval: when the anode was polarized to 0.6~0.8 V vs. SCE, the obtained current of anode cells with CA was around 320 to 220 mA/m², much higher than those with NA, the difference was about an order of magnitude. The difference in catalytic efficiency also resulted in a difference in depolarizing effects: the open circuit potential of anode cells with CA was generally within the range of 0.13 to 0.23 V vs. SCE, while that of reference cells was around 0.64 V vs. SCE. This result indicates that after long term energization, a minor degree of difference in primary anode degradation can be expected due to the variation of secondary anode material (cementitious overlay). The presence of CA in anode cell contributes to the maintenance of catalytic activity of MMO-Ti anode in low polarization state (0.6~0.8 V vs. SCE).

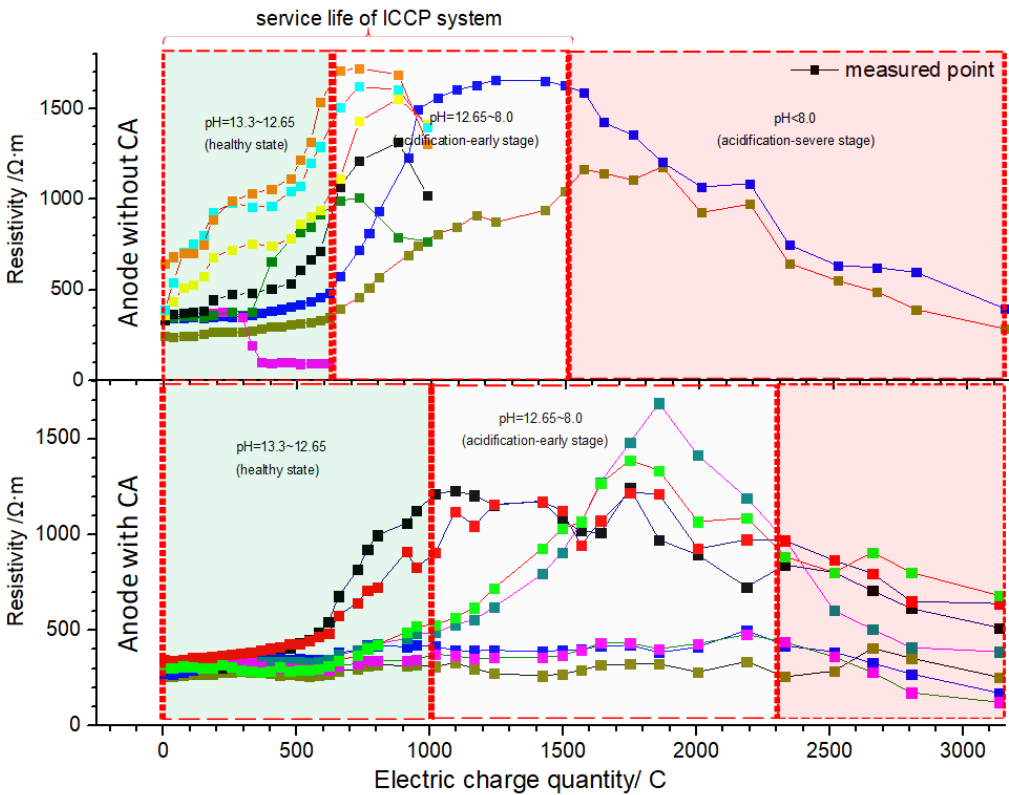


Figure 10: Electrical resistivity of concrete bridge in simulated ICCP test cells

The electrical resistivity of the concrete bridge in the ICCP cells is shown in Figure 10. Combining with the previous cell voltage monitored results as presented in Figure 6, the alteration in resistivity of concrete bridge can be the primary reason to the variation in cell voltage in constant current operating condition. Firstly, the variation in the monitored resistivity can be attributed to the micro-scaled structural difference in concrete bridge: the concrete bridge was only 2 cm in thickness with an exposure area of 12 cm², therefore, the heterogeneity of concrete will be amplified between each test cell. Generally, when ICCP is applied, the main cathodic reaction (as shown in Equation 6) on the surface of the reinforcement would increase OH⁻ concentration in the pore solution of concrete matrix, at the opposite site, Ca²⁺ together with Na⁺ and K⁺ would also diffused to the cathode site under electric field, and precipitate salt crystals like Ca(OH)² can be expected to be occurred in the pore structures within concrete bridge, and the accumulation of this effect would further lead to a refined pore structure of concrete bridge. With the refinement of the pore structure, the migration rate of the ions decreased, resulted in the increased resistivity of the concrete bridge as presented in Figure 9: the concrete resistivity of all test simulated ICCP cells increased in the early stage (around 700 C of accumulated electric charge quantity), known as the secondary beneficial effects.



However, when the treatment time was prolonged, the resistivity of the concrete bridge gradually decreased. During ICCP treatment, the anodic reactions as shown in Equations 1 - 3 consumed OH⁻ in simulated pore solution in the vicinity of primary Ti mesh anode. After the pH drop, the solubility equilibrium between hydration products and pore solution was broken, leading to the dissolution of CH and other hydration products and subsequently more porous microstructure of concrete matrix. Therefore, at later stages, for some test cells, the resistivity of concrete bridge was reduced. Further, as presented in Figure 9, the negative effect induced by the acidification damage was significantly postponed in the presence of CA in the anode cell, which indicates the significance of the acidification inhibition to the global secondary beneficial effects within ICCP system, and the effectiveness of CA in the mitigation of anode deterioration.

4 Conclusions

In this study, a novel type of anode embedding mortar was designed and prepared based on lightweight functional aggregates, obtained by impregnation with alkaline agar gel, intended to provide a large alkaline buffer. Mortar with the functional aggregate or with normal aggregate were subjected to accelerated ICCP tests with electrodes in anode and cathode chambers filled with simulated pore solution and the aggregate, while the acidification of the anode solution was tested. According to the experimental results, the main conclusions can be summarized as follows:

- The resistivity of the conductive mortar was in the range from 15.3 to 14.2 Ωm in the presence of 40~45 vol.% of CA at a curing age of 28 days, at a much lower level than mortar prepared with normal aggregate (river sand, which had a resistivity of about 50 Ωm).
- The acidification in the anode system could be effectively slowed down in the presence of CA. The alkaline buffer capacity was improved by 53%, 91% and 132% in presence of 15, 25 and 40 vol.% of CA compared to reference specimens.
- Due to the high structural stability of MMO-Ti anode, no distinct difference in catalytic performance can be expected after the acidification of anode cells. However, the presence of CA contributes to the maintenance of alkaline environment during the operation and benefits to the catalytic environment. Compared with acidized anode without CA, a lower polarization potential and a relatively slighter acidification damage in cementitious overlay can be expected.

Acknowledgements

This work was financially supported by National Key Research and Development Program of China (Project No.2017YFB0309904) and National Natural Science Foundation of China (No. 51572088). Their financial supports are gratefully acknowledged.

Literature

Weale, C.J., *Cathodic Protection of Reinforced Concrete: Anodic process in cements and related electrolytes*, Ph.D. thesis, Aston University, 1992.

Page CL., Sergi G., Development in cathodic protection applied to reinforced concrete. *Journal of Materials in Civil Engineering* 2000;12(1):8-15.

- Pedefferri P., Cathodic protection and cathodic prevention. *Construction and Building Materials*. 1996;10(5):391-402.
- Bertolini L., Elsener B., Pedefferri P., Polder R., *Corrosion of Steel in Concrete: Prevention, Diagnosis, Repair*. Weinheim: WILEY-VCH Verlag GmbH & Co. KGaA; 2013.
- Koleva DA., *Corrosion and protection in reinforced concrete Pulse cathodic protection: an improved cost-effective alternative* Ph.D. thesis, Delft University of Technology, the Netherlands, 2007.
- Bennett JE., Bartholomew JJ, Bushman JB, Clear KC, Kamp RN, Swiat WJ., Cathodic Protection of Concrete Bridges: A Manual of Practice. Washington, DC: Strategic Highway Research Program. National Academy of Science, 1993.
- Peelen WHA., Polder RB., Redaelli E., Bertolini L., Qualitative model of concrete acidification due to cathodic protection. *Materials and Corrosion*. 2008;59(2):81-9.
- Monteiro AO., Cachim PB., Costa PMFJ., Electrical Properties of Cement-based Composites Containing Carbon Black Particles. *Materials Today: Proceedings*. 2015;2(1):193-9.
- Yehia SA., Tuan C, Y., Ferdon D., Chen B., Conductive concrete overlay for bridge deck deicing: Mixture proportioning, optimization, and properties. *ACI Mater J*. 2000;97(2):172-81.
- Xu J., Yao W., Electrochemical studies on the performance of conductive overlay material in cathodic protection of reinforced concrete. *Construction and Building Materials*. 2011;25(5):2655-62.
- Garcés P., Zornoza E., Alcocel EG., Galao Ó., Andión LG., Mechanical properties and corrosion of CAC mortars with carbon fibers. *Construction and Building Materials*. 2012;34:91-6.
- Gao J., Wang Z., Zhang T., Zhou L., Dispersion of carbon fibers in cement-based composites with different mixing methods. *Construction and Building Materials*. 2017;134:220-7.
- Bertolini L., Bolzoni F., Pastore T., Pedefferri P., Effectiveness of a conductive cementitious mortar anode for cathodic protection of steel in concrete. *Cement and Concrete Research*. 2004;34(4):681-94.
- ASTM G57-06(2012), Standard Test Method for Field Measurement of Soil Resistivity Using the Wenner Four-Electrode Method. ASTM International; 2012.
- McLachlan DS., Blaszkiewicz M., Newnham RE., Electrical Resistivity of Composites. *Journal of the American Ceramic Society*. 1990;73.
- Adenot F., Buil M., Modelling of the corrosion of the cement paste by deionized water. *Cement and Concrete Research*. 1992;22(2):489-96.